Molecular Ecology (2008) **17**, 885–901 doi: 10.1111/j.1365-294X.2007.03618.x

Replaying the tape: recurring biogeographical patterns in Cape Verde *Conus* after 12 million years

REGINA L. CUNHA,*† MANUEL J. TENORIO,‡ CARLOS AFONSO,† RITA CASTILHO† and RAFAEL ZARDOYA*

**Departamento de Biodiversidad y Biología Evolutiva, Museo Nacional de Ciencias Naturales-CSIC, José Gutiérrez Abascal, 2, 28006 Madrid, Spain, †CCMAR, Campus de Gambelas-Universidade do Algarve, 8005-139 Faro, Portugal, ‡Facultad de Ciencias, Universidad de Cadiz, 11510 Puerto Real, Cádiz, Spain*

Abstract

Isolated oceanic islands are excellent natural laboratories to test the relative role of historical contingency and determinism in evolutionary diversification. Endemics of the marine venomous snail *Conus* in the Cape Verde archipelago were originated from at least two independent colonizations of 'small' and 'large' shelled species separated by 12 million years. In this study, we have reconstructed phylogenetic relationships within large-shelled *Conus* (*C. ateralbus*, *C. pseudonivifer*, *C. trochulus*, and *C. venulatus*) based on mitochondrial *cox1* and *nad4* haplotype sequences. The reconstructed molecular phylogeny revealed three well-supported and relatively divergent clades (A, B, and C) that do not correspond to current species classification based on shell colour and banding patterns. Clade A grouped specimens assigned either to *C. pseudonivifer* or *C. trochulus*, clade B is composed of specimens assigned to *C. venulatus*, and clade C comprises specimens assigned either to *C. venulatus* or *C. ateralbus*. Geometric morphometric analyses found significant differences between the radular teeth shape of *C. pseudonivifer*/*C. trochulus* and *C. venulatus*/*C. ateralbus*. In clades A and B, northwestern Boavista and Maio specimens cluster together to the exclusion of eastern Boavista samples. In Sal, populations form a monophyletic island assemblage (clade C). The large-shelled *Conus* have remarkably replicated biogeographical patterns of diversification of small-shelled *Conus*. Similar selective forces (i.e. nonplanktonic lecithotrophy with limited larval dispersal and allopatric diversification) together with repeated instances of low sea level stands during glacial maxima that allowed connection between islands, have overcome the effect of historical contingency, and explain the observed recurring biogeographical patterns.

Keywords: Cape Verde, contingency, *Conus*, determinism, geometric morphometrics, phylogeographic patterns

Received 22 June 2007; revision accepted 25 October 2007

Introduction

The origin and causes of the great species diversity observed in oceanic archipelagos are among the most intriguing questions in evolutionary biology (Emerson 2002). The remarkable number of closely related endemic species found in oceanic islands is generally believed to be the result of single or multiple successful colonizations followed by the diversification of founding populations through vicariant events and/or niche adaptation. Although there are numerous examples of how such evolutionary processes have shaped island terrestrial biota (e.g. Emerson *et al*. 1999; Gillespie 2004; Losos 2004), fewer examples are known regarding marine species diversification in oceanic archipelagos (Cunha *et al*. 2005). For instance, while the impacts of Pleistocene climate changes upon the genetic diversity and biogeography of continental (Taberlet *et al*. 1998; Hewitt 2000; Barnosky *et al*. 2004) and island (Richman *et al*. 1988; Millien-Parra & Jaeger 1999; Jordan *et al*. 2005) terrestrial fauna are becoming well understood, little is known regarding the glacial effects on speciation and diversification of marine taxa. However, it is well known that eustatic sea-level fluctuations modified in the

Correspondence: Regina L. Cunha, Fax: +351 289 800069; E-mail: rcunha@ualg.pt

past both coastline shape and distances among islands (Graham *et al*. 2003), and therefore must have affected the evolutionary patterns of associated marine fauna. The evolutionary effects of changes in other intrinsic aspects of the biology of marine species such as, e.g. transitions in larval feeding mode (i.e. planktotrophy to lecithotrophy; Strathmann 1985; Scheltema 1989) also merit more attention.

The marine venomous snail genus *Conus* (Gastropoda) has remarkably radiated in Cape Verde islands, where the described species represent about 10% of the global diversity within the genus (Monteiro *et al*. 2004; Duda & Kohn 2005). The radiation of *Conus* in Cape Verde represents a particularly suitable model to understand the processes underlying marine species diversification on islands. The molecular phylogeny of this group revealed the existence of two main clades (Duda & Rolán 2005) including 'small' and 'large' shelled species, respectively (Cunha *et al*. 2005). The phylogenetic relationships among small-shelled *Conus* are fairly known whereas those within the large-shelled clade await resolution (Cunha *et al*. 2005). The ancestor of the small-shelled clade colonized Cape Verde around 16.5 million years ago (Ma) whereas the ancestor of the large-shelled clade arrived around 4.6 Ma (Cunha *et al*. 2005). The successful colonization of large-shelled *Conus* in a more recent period was likely possible because they could access to food resources not exploited by the small-shelled clade species (Leviten 1978). The large difference in the arrival date of the ancestors of both clades allowed greater species diversification within the small-shelled clade, whereas speciation process in the large-shelled clade is still incipient. Both clades occur in the easternmost islands (Sal, Boavista, Santiago, and Maio) of the archipelago of Cape Verde whereas only small-shelled *Conus* are found in the remaining islands (Rolán 1992; Monteiro *et al*. 2004). In the easternmost islands, where both clades coexist, the small-shelled *Conus* species from Sal form a monophyletic group but not those from Boavista and Maio (Cunha *et al*. 2005). The limited dispersal capacity of the nonplanktonic lecithotrophic larvae of small-shelled *Conus* together with eustatic sea level changes are believed to have driven the diversification of the group (Cunha *et al*. 2005). Three successive low stands of sea level at 10.5, 5.5 and 3.8 Ma, respectively (Haq *et al*. 1987), allowed colonization of the different islands of the Cape Verde archipelago, and produced monophyletic island species assemblages (Cunha *et al*. 2005). Posterior high sea-level stages isolated the islands, and promoted allopatric speciation. Connectivity between Maio and Boavista was enhanced by the relatively shallow channel (–100 m; Carta Hidrográfica do Arquipélago de Cabo Verde, 1971) between both islands leading to nonmonophyletic assemblages of small-shelled *Conus* in these islands.

The endemic large-shelled *Conus* of Cape Verde are classified into four recognized species: *C. venulatus* Hwass, 1792, *C. trochulus* Reeve, 1844, *C. ateralbus* Kiener, 1845, and *C. pseudonivifer* Monteiro, Tenorio & Poppe, 2004. These species occur only in the four easternmost islands of the archipelago (Fig. 1): *C. ateralbus* is restricted to Sal, *C. trochulus* is found only in Boavista, *C. pseudonivifer* occurs in Boavista, Santiago, and Maio, whereas *C. venulatus* presents the widest distribution occurring in all four islands (Rolán 1992). These species were diagnosed mostly based on shell colour and banding patterns. However, these phenotypic traits have been found to be highly variable at the intraspecific level (see Fig. 1), which in turn makes species assignment problematic, and in many cases misleading.

The Cape Verde endemics of the large-shelled clade offer an exceptional opportunity to gain insights into the evolutionary processes that lead to diversification of marine species on islands. In particular, we can test whether the ongoing diversification of the ancestor of the large-shelled clade, may be replicating the same biogeographical pathways followed by the small-shelled clade almost 12 million years (Myr) before or whether historical contingency may have dominated the evolutionary process rendering disparate diversification patterns. Testing among these competing hypotheses requires a robust phylogenetic framework. Therefore, the specific goals of this study were: (i) to infer the phylogenetic relationships and phylogeographic patterns within the large-shelled clade using mitochondrial sequence data, (ii) to test the validity of shell colour and banding pattern as diagnostic characters for species determination, (iii) to explore whether it is possible to delimit discrete groups within the large-shelled clade using geometric morphometrics of the shell and radula shape, and (iv) to date major cladogenetic events within the clade.

Materials and methods

Taxon sampling, DNA sources and extraction

A total of 200 specimens of large-shelled Cape Verde *Conus* belonging to the four currently recognized species were collected from 16 locations in Sal, Boavista and Maio between 2003 and 2006 (sample locations are shown in Fig. 1 and Table 1). Despite *C. pseudonivifer* and *C. venulatus* have been also cited in Santiago, we failed to collect any specimen of these species in our two visits to the island in the fall of 2005 and spring of 2006, respectively. The sampling rendered a total of 25 populations (i.e. specimens with the same shell colour and banding phenotype collected in the same location) for further analyses. An average of eight specimens was collected per population. Larger samplings were not possible mostly due to scarceness of specimens at the different sites. Taxonomy followed Rolán (1992) and Monteiro *et al*. (2004). All specimens were preserved in 98%

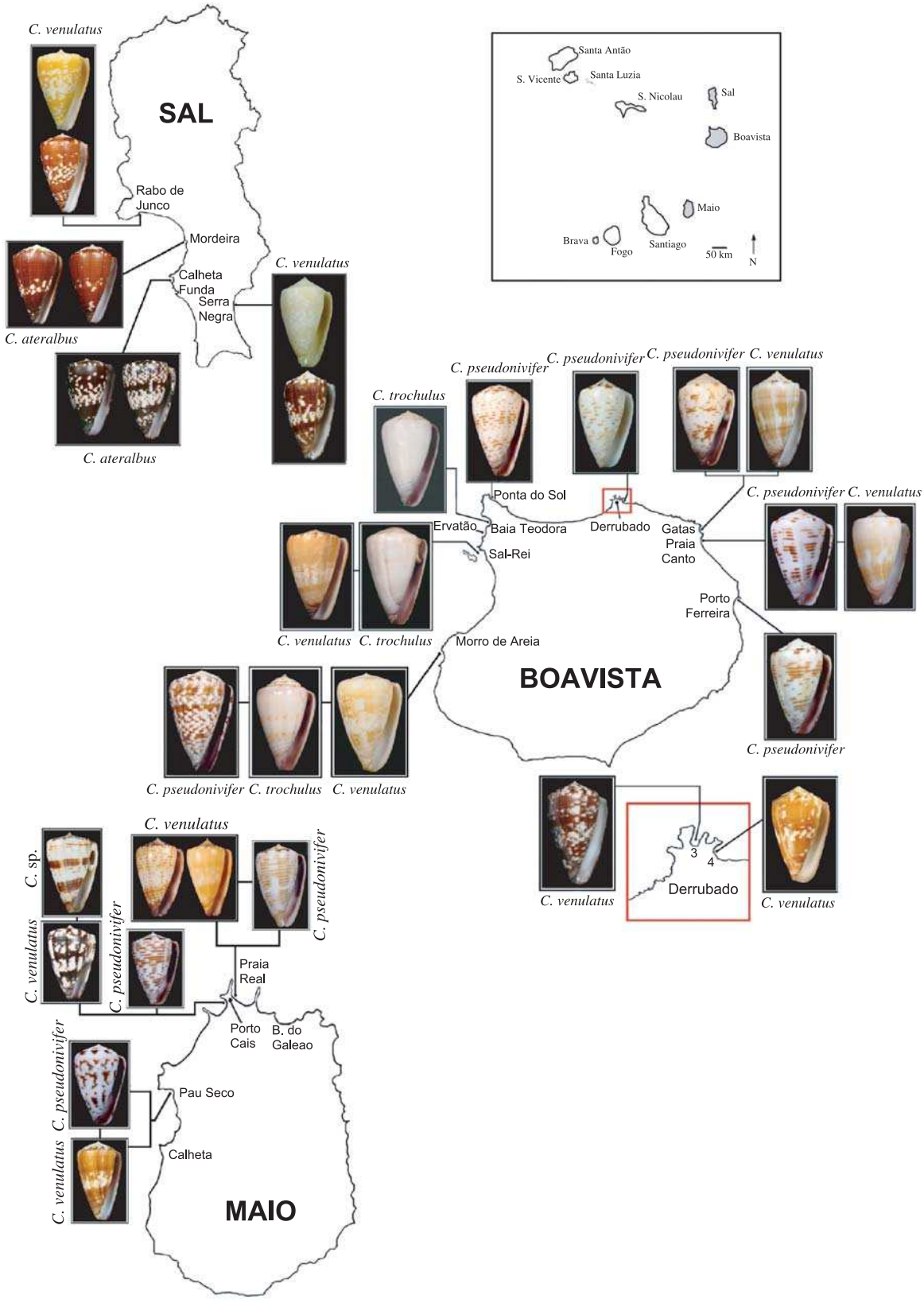

Fig. 1 Map of the Cape Verde archipelago. Sampled islands are coloured in grey. Distribution and shell banding patterns of the large-shelled populations of Cape Verde *Conus* in the islands of Boavista, Maio, and Sal are shown.

Table 1 List of species (as identified by their shell banding phenotypes) and respective haplotypes. Sampling sites surveyed in this study, number of individuals per sampling site, GenBank Accession numbers and respective vouchers

Conus	Haplotype	Island	Bay	N/ location	GenBank Accession no. *cox1*	GenBank Accession no. *nad4*	Voucher no.
C. ateralbus	H1	Sal	Calheta Funda	1	EF076247	EF076447	MNCN/ADN:21088
C. ateralbus	H2	Sal	Calheta Funda	3	EF076248–50	EF076448–50	MNCN/ADN:21089–91
C. ateralbus	H3	Sal	Calheta Funda	1	EF076251	EF076451	MNCN/ADN:21092
C. ateralbus	H4	Sal	Calheta Funda	8	EF076252–59	EF076452–59	MNCN/ADN:21093–21100
C. ateralbus	H5	Sal	Calheta Funda	2	EF076260–61	EF076460–61	MNCN/ADN:21101–02
C. ateralbus	H6	Sal	Calheta Funda	1	EF076262	EF076462	MNCN/ADN:21103
C. ateralbus	H7	Sal	Calheta Funda	1	EF076263	EF076463	MNCN/ADN:21104
C. ateralbus	H8	Sal	Calheta Funda	7	EF076264–70	EF076464–70	MNCN/ADN:21105–11
C. venulatus	H9	Sal	Rabo Junco	4	EF076271–74	EF076471–74	MNCN/ADN:21112–15
C. venulatus	H10	Sal	Rabo Junco	1	EF076275	EF076475	MNCN/ADN:21116
C. venulatus	H11	Sal; Boavista	Serranegra; Derrubado 3	11; 2	EF076276–86; EF076287–88	EF076476–86; EF076487–88	MNCN/ADN:21117–27;28–29
C. venulatus	H12	Boavista	Morro Areia	1	EF076289	EF076289	MNCN/ADN:21130
C. venulatus	H13	Boavista	Morro Areia	1	EF076290	EF076290	MNCN/ADN:21131
C. pseudonivifer	H14	Boavista; Maio	Morro Areia; Praia Real	3; 8	EF076291–93; EF076298–305	EF076491–93; EF076498–505	MNCN/ADN:21132–34;35–42
C. trochulus	H14	Boavista	Sal Rei	4	EF076294–7	EF076494–97	MNCN/ADN:21143–46
C. pseudonivifer	H15	Boavista	Morro Areia	1	EF076306	EF076506	MNCN/ADN:21147
C. venulatus	H16	Boavista	Sal Rei: Derrubado 4	3; 6	EF076307–9; EF076310–15	EF076507–9; EF076510–15	MNCN/ADN:21148–50;51–56
C. venulatus	H17	Boavista	Sal Rei	2	EF076316–17	EF076516–17	MNCN/ADN:21157–58
C. venulatus	H18	Boavista	Sal Rei	3	EF076318–20	EF076510–20	MNCN/ADN:21159–61
C. pseudonivifer	H18	Boavista	Ponta Sol	7	EF076321–27	EF076521–27	MNCN/ADN:21162–68
C. venulatus	H19	Boavista	Sal Rei	3	EF076328–30	EF076528–30	MNCN/ADN:21169–71
C. venulatus	H20	Boavista	Praia Canto	2	EF076331–32	EF076531–32	MNCN/ADN:21172–73
C. venulatus	H21	Boavista	Praia Canto	1	EF076333	EF076533	MNCN/ADN:21174
C. venulatus	H22	Boavista	Praia Canto	1	EF076334	EF076534	MNCN/ADN:21175
C. venulatus	H23	Boavista	Praia Canto	1	EF076335	EF076535	MNCN/ADN:21176
C. venulatus	H24	Boavista	Praia Canto	1	EF076336	EF076536	MNCN/ADN:21177
C. venulatus	H25	Boavista	Derrubado 3; Derrubado 4	1; 11	EF076337; 38–48	EF076537–48	MNCN/ADN:21178–89
C. venulatus	H26	Boavista	Derrubado 4	1	EF076349	EF076549	MNCN/ADN:21190
C. venulatus	H27	Boavista	Derrubado 4	1	EF076350	EF076550	MNCN/ADN:21191
C. venulatus	H28	Boavista	Derrubado 4	1	EF076351	EF076551	MNCN/ADN:21192
C. venulatus	H29	Maio	Pau Seco	1	EF076352	EF076552	MNCN/ADN:21193
C. venulatus	H30	Maio	Pau Seco; Porto Cais	1; 5	EF076353–58	EF076553–58	MNCN/ADN:21194;95–99
Conus sp.	H30	Maio	Porto Cais	1	EF076359	EF076559	MNCN/ADN:21200
C. venulatus	H31	Maio	Porto Cais	1	EF076360	EF076560	MNCN/ADN:21201
C. venulatus	H32	Maio	Praia Real	1	EF076361	EF076561	MNCN/ADN:21202
C. venulatus	H33	Maio	Praia Real	1	EF076362	EF076562	MNCN/ADN:21203
C. trochulus	H34	Boavista	Sal Rei	1	EF076363	EF076563	MNCN/ADN:21204
C. trochulus	H35	Boavista	Morro Areia	4	EF076364–67	EF076564–67	MNCN/ADN:21205–8
C. pseudonivifer	H35	Boavista	Morro Areia	2	EF076368–69	EF076568–69	MNCN/ADN:21209–10
C. trochulus	H36	Boavista	Teodora; Ervatão	6	EF076370–75	EF076570–75	MNCN/ADN:21211–16
C. trochulus	H37	Boavista	Teodora; Ervatão	11	EF076376–86	EF076576–86	MNCN/ADN:21217–227
C. pseudonivifer	H37	Maio	Praia Real	1	EF076387	EF076587	MNCN/ADN:21228
C. trochulus	H38	Boavista	Teodora	1	EF076388	EF076588	MNCN/ADN:21229
C. trochulus	H39	Boavista	Ervatão	2	EF076389–90	EF076589–90	MNCN/ADN:21230–31
C. trochulus	H40	Boavista	Ervatão	1	EF076391	EF076591	MNCN/ADN:21232
C. pseudonivifer	H41	Boavista	Porto Ferreira; Gatas; Praia Canto	8; 1; 11	EF076392–99; EF076411; EF076400–10	EF076592–99; EF076611; EF076600–10	MNCN/ADN:21233–40;41;42–52
C. venulatus	H42	Boavista	Morro Areia	1	EF076412	EF076612	MNCN/ADN:21252

Table 1 *Continued*

Conus	Haplotype	Island	Bay	N/ location	GenBank Accession no. *cox1*	GenBank Accession no. *nad4*	Voucher no.
C. pseudonivifer	H43	Boavista	Derrubado 4	8	EF076413–20	EF076613–20	MNCN/ADN:21253–61
C. pseudonivifer	H44	Boavista	Derrubado 4	2	EF076421–22	EF076621–22	MNCN/ADN:21262–63
C. pseudonivifer	H45	Boavista	Ponta Sol	1	EF076423	EF076623	MNCN/ADN:21264
C. pseudonivifer	H46	Boavista	Ponta Sol	1	EF076424	EF076624	MNCN/ADN:21265
C. pseudonivifer	H47	Maio	Pau Seco	13	EF076425–37	EF076625–37	MNCN/ADN:21264–78
C. pseudonivifer	H48	Maio	Porto Cais	5	EF076438–42	EF076638–42	MNCN/ADN:21279–83
C. pseudonivifer	H49	Maio	Praia Real	1	EF076443	EF076643	MNCN/ADN:21284
C. pseudonivifer	H50	Maio	Praia Real	1	EF076444	EF076644	MNCN/ADN:21285
Conus sp.	H51	Maio	Porto Cais	1	EF076445	EF076645	MNCN/ADN:21286
Conus sp.	H52	Maio	Porto Cais	1	EF076446	EF076646	MNCN/ADN:21287

Table 2 Polymerase chain reaction primers used for amplification of mitochondrial *cox1*and *nad4* genes

Primer	No.
cox1	
LCO1490*	
HCO2198*	
VEN_COI-F (CCAGGTGCTTTGCTTGGAGATG)	1
VEN_COI-R (GGTAAAGATAAAAGAAGTAAAATAG)	2
nad4	
Conus_ND4-F (CCTGGTCTTTAGCTCTGCTAAG)	3
Conus_H-R (GCTGACGTTTTAGTATTAAAC)	4
VEN_ND4-F (GATGTGATTCAATATCTCTTGC)	5
VEN_ND4-R (TATTAACAGGAACTCAGTG)	6

*(Folmer *et al*. 1994).

ethanol, and total genomic DNA was extracted from muscle tissue using either a standard phenol–chloroform DNA extraction protocol with cetyltrimethyl ammonium bromide (CTAB) (Doyle & Doyle 1987), or commercial extraction kits (DNeasy Extraction Kit, QIAGEN; ChargeSwitch gDNA Micro Tissue Kit, Invitrogen).

PCR amplification and sequencing

Universal primers from Folmer *et al*. (1994) were used in polymerase chain reactions (PCRs) to amplify in a few specimens about 600 base pairs (bp) of mitochondrial cytochrome oxidase C subunit 1 (*cox1*). Subsequent PCRs were carried out using *Conus* specific primers (primers 1 and 2, Table 2) to amplify a 404-bp fragment. The same optimization procedure was followed for the PCR amplification of NADH dehydrogenase subunit 4 (*nad4*). An initial fragment of approximately 1400 bp was obtained with primers 3 and 4 (Table 2). Subsequent PCRs were carried out using internal primers 5 and 6 (Table 2) to amplify a 1040-bp fragment. All PCR amplifications were conducted in 25 μL reactions containing 1× PCR buffer, 0.2 mM of each dNTP, 0.2 μM of each primer, 1 μL of template DNA, and *Taq* DNA polymerase (1 U, CLONTECH-TaKaRa), using the following programme: one cycle of 1 min at 95 °C, 35 cycles of 30 s at 95 °C, 30 s at 54 °C, and 90 s at 68 °C, and finally, one cycle of 5 min at 68 °C. PCR products were purified with an ethanol/sodium acetate precipitation, and directly sequenced using the corresponding PCR primers. Samples were sequenced in an automated DNA sequencer (ABI PRISM 3700) using the BigDye Deoxy Terminator cycle-sequencing kit (Applied Biosystems) following the manufacturer's instructions. Sequences were deposited in GenBank under the Accession numbers given in Table 1.

Phylogenetic analyses

DNA sequences from mitochondrial *cox1* and *nad4* genes were aligned with CLUSTAL_X version 1.81 (Thompson *et al*. 1997) using the default settings. Identical haplotypes were collapsed with the program COLLAPSE version 1.2 (Posada 2004). The Akaike information criterion (Akaike 1973) implemented in MODELTEST 3.7 (Posada & Crandall 1998) selected TrN + I as the evolutionary model that best fit the data set (A: 0.26, C: 0.17, G: 0.17, T: 0.40; [A-C] = 1, [A-G] = 26.9, [A-T] = 1, [C-G] = 1, [C-T] = 19.7; I = 0.84). These settings were used in the maximum likelihood (ML) analysis that was performed with PHYML (Guindon & Gascuel 2003). The robustness of the inferred trees was tested by nonparametric bootstrapping (BP) using 500 pseudoreplicates. Bayesian inferences (BI) were performed using MRBAYES version 3.1.2 (Ronquist & Huelsenbeck 2003) by Metropolis coupled Markov chain Monte Carlo (MCMCMC) sampling for 1 000 000 generations (four

simultaneous MC chains; sample frequency 100) under the GTR + I model. Burn-in occurred within the first 50 000 generations. Two independent runs were performed to reduce chances of selecting a local but not a global optimum. The robustness of the inferred trees was tested using Bayesian posterior probabilities (BPP).

Network analysis

Haplotype genealogies within each of the three main clades recovered in the phylogenetic analyses were reconstructed with TCS version 1.2.1 (Clement *et al*. 2000) 2 Templeton *et al*. (1992). Pairwise distance values for all haplotypes were estimated in order to define the limits of parsimony in constructing networks above the 95% level. All haplotypes were connected in a network using these limits (except H41, see Results).

Population genetic structure

Haplotype and nucleotide diversities were estimated with DNASP version 3.14 (Rozas *et al*. 2003). Hierarchical genetic structuring was tested in clades A and B of the recovered molecular phylogeny by assessing the relative contribution among groups (northwest Boavista vs. eastern Boavista vs. Maio), within groups and within population components for partitions of total molecular variance (AMOVA) (Excoffier *et al*. 1992) using ARLEQUIN version 3.0 (Excoffier *et al*. 2005) and 20 000 permutations. Sequence divergence between haplotypes was estimated under the TrN evolutionary model.

Divergence time estimation

A likelihood ratio test (Huelsenbeck & Crandall 1997) between ML trees inferred with and without a clock constraint was performed using PAUP* 4.0b10 (Swofford 1998). The molecular clock hypothesis was rejected, and thus, divergence times were estimated following a Bayesian 'relaxed-clock' approach (Kishino *et al*. 2001). This procedure is outlined in Cunha *et al*. (2005). *Conus borgesi* (belonging to the small-shelled clade) was used as outgroup. The prior value for the expected number of time units between the tip and the root (rttm) and the standard deviation were both set to 55, where 1 time unit represents 1 Myr. This value was obtained based on the earliest *bona fide* fossil record of *Conus* (see Cunha *et al*. 2005). The mean and standard variation of prior distribution for rate at root node (rtrate) was set to 0.0004 (estimated as in Cunha *et al*. 2005). Due to the lack of dated fossils of Cape Verde *Conus*, we used age estimates from Cunha *et al*. (2005) as calibration points. Two divergence dates were used as minimum age constraints: *C. ateralbus* (3.31–1.97 Myr) and *C. trochulus* (0.198–0.72 Myr).

Morphometric characterization of shell and radula variability

A geometric morphometric analysis of the shell shape was performed on 174 specimens corresponding to 15 populations (all except *C. venulatus* from Junco and Pau Seco; *C. trochulus* from Ervatão, Morro de Areia and Sal Rei; *C. pseudonivifer* from Morro de Areia and Ponta do Sol). The exclusion of the abovementioned populations was due to insufficient number of specimens, or shell erosion. Only adult specimens with lengths between 27 mm and 45 mm (in order to avoid the effects of allometry) and well-preserved spires were selected. Specimens were individually photographed in ventral position using a digital camera mounted in a perpendicular angle to the shell. Pictures were taken at a distance of 35–40 cm in order to minimize the image distortion and parallax error. Taking several pictures of the same specimen ensured the reproducibility of the measurements by checking that the deviation in landmark positioning was minimal. A total of 15 points were selected to capture shell shape (Table 3). Points 1, 2 and 5–11 were treated as landmarks, whereas the remaining ones were treated as semilandmarks. These points cover most of the ratios used for classical morphometric characterization of *Conus* shell morphometry (Kohn & Riggs 1975).

In addition, radular teeth, which have been shown to be particularly informative for species identification in *Conus* (Rolán & Raybaudi-Massilia 1994, 2002; Kohn *et al*. 1999), were also subjected to geometric morphometric analysis. Radular tooth morphology was examined in a total of 107 specimens from 21 populations of *Conus* (all except *C. pseudonivifer* from Porto Cais and Gatas, *C. venulatus* from Morro de Areia, and *Conus* sp. from Porto Cais). For each population, typically between four and seven *Conus* specimens were selected (see Appendix). Landmark positioning was performed in one tooth per specimen. Soft parts of each individual were digested with KOH, and the radula was extracted with tweezers. Digital images were taken under an optical microscope. The radular teeth of the *Conus* under study are hollow tubular, dart-like structures. Radular teeth were positioned so as that the barb and the blade were clearly visible, which allowed direct comparison among different teeth in a constant and reproducible manner. All of the radular teeth included in this study were comparable in size (between 0.65 mm and 0.85 mm) and of adult *Conus* specimens in order to avoid possible effects of allometry. Except for the very early stages corresponding to juvenile states, the shape of the tooth in the adult *Conus* is essentially constant and does not depend much on size (Rólan *et al*. 2002). Differences in radular tooth mean size between taxa groups (*C. ateralbus*, 0.69 mm; *C. venulatus*, 0.72 mm; *C. trochulus*, 0.78 mm; and *C. pseudonivifer*, 0.80 mm) were not significant ($P > 0.05$),

Table 3 Selected points for capturing the shape of the shell and each radular tooth

	Points	Trait
Shell		
	1 and 2	Apex of the spire and tip of the siphonal canal
	3 and 4	Maximum width of the shell
	5 to 11	Intersection of each whorl of the spire with the profile
	12 and 14	Intersections with the left profile of the shell with the perpendiculars to the segment that connects landmarks 6 and 2
	13 and 15	Intersection of the perpendiculars to the segment that connects landmarks 5 and 2 with the external profile of the aperture of the shell
Radula		
	1 and 2	Main axis (ends of radular tooth)
	3	Shape of the barb
	4 and 5	Maximum width of the apical portion of the tooth
	6	Intersection of the blade with the apical portion
	7 and 8	Waist of the radular tooth
	9 and 10	Height of the maximum width of the shaft
	11 and 12	Maximum width of the base
	13 to 16	Folds of the shaft
	17	Top of serration

except for the difference between the mean sizes of the radular teeth of *C. pseudonivifer* and *C. ateralbus* (t = 2.83, P = 0.01).

Teeth were digitized using TPSDIG2 (Rohlf 2005). A total of 17 points were selected for capturing the shape of each tooth (Table 3). These points cover most of the ratios used for classical morphometric characterization of the vermivorous radular tooth (Rolán & Raybaudi-Massilia 1994, 2002; Kohn *et al*. 1999). Points 1–4, 6–8, and 13–17 were treated as landmarks, whereas the remaining ones were treated as semilandmarks.

Once all shells and radular teeth were digitized, the semilandmarks were allowed to relax by sliding (Zelditch *et al*. 2004). Shell and radular tooth semilandmarks were allowed to slide to the position that minimizes the squared Procrustes distance between the form of the shell or the form of the radular tooth of a given specimen, and the consensus reference form for all analysed shells or radular teeth, respectively. This was accomplished using the program TPSRELW, version 1.42 (Rohlf 2005). Landmarks were aligned by a standard generalized least squares (GLS) procedure. The within-population Procrustes distances were calculated as the mean (with its corresponding standard deviation) of the shell or radular tooth pairwise Procrustes distance matrices, respectively, as generated by the program COORDGEN6 (Sheets 2003–2005). The pairwise Procrustes distances between populations based upon either shell or radular tooth morphometry were obtained with the program TWOGROUP6 (Sheets 2003–2005) using resampling methods (400 bootstraps) in order to circumvent problems related to the adjustment of the correct number of degrees of freedom when semilandmarks are used. The significance of the Goodall's F test was assessed by a bootstrapped F test. The 95% probability interval and standard error were also determined by bootstrapping. Partial warps and their principal components (relative warps) were computed using the program PCAGEN6P (Sheets 2003–2005) included in the IMP software suite. Canonical variate analysis (CVA) was performed using the program CVAGEN6N (Sheets 2003–2005). These programs were also used for generating the two-dimension (2D) scatter plots and the corresponding deformation grids and vectors. The MANOVA tests were performed with MANOVABOARD (Sheets 2003–2005).

Results

Phylogenetic analysis and divergence dates

The partial sequences of the mitochondrial *cox1* and *nad4* genes were aligned and combined into a single data set of 1444 positions. Of these, 1334 were invariant, and 90 were parsimony-informative. The reconstructed unrooted ML tree (–ln L = 2947.66) is depicted in Fig. 2. The Bayesian inference analysis yielded an identical topology (–ln L = 3025.46). According to the recovered phylogenetic relationships, large-shelled *Conus* from Cape Verde could be grouped into three well-supported and relatively divergent clades (A, B, and C). Three of the four recognized species as diagnosed based on shell colour and banding patterns are not monophyletic, and only *C. ateralbus* is recovered as a natural group. Clade A, which is supported by maximal BP and BPP values, grouped haplotypes corresponding to *C. pseudonivifer* and *C. trochulus* shell banding phenotypes. Phylogenetic relationships within

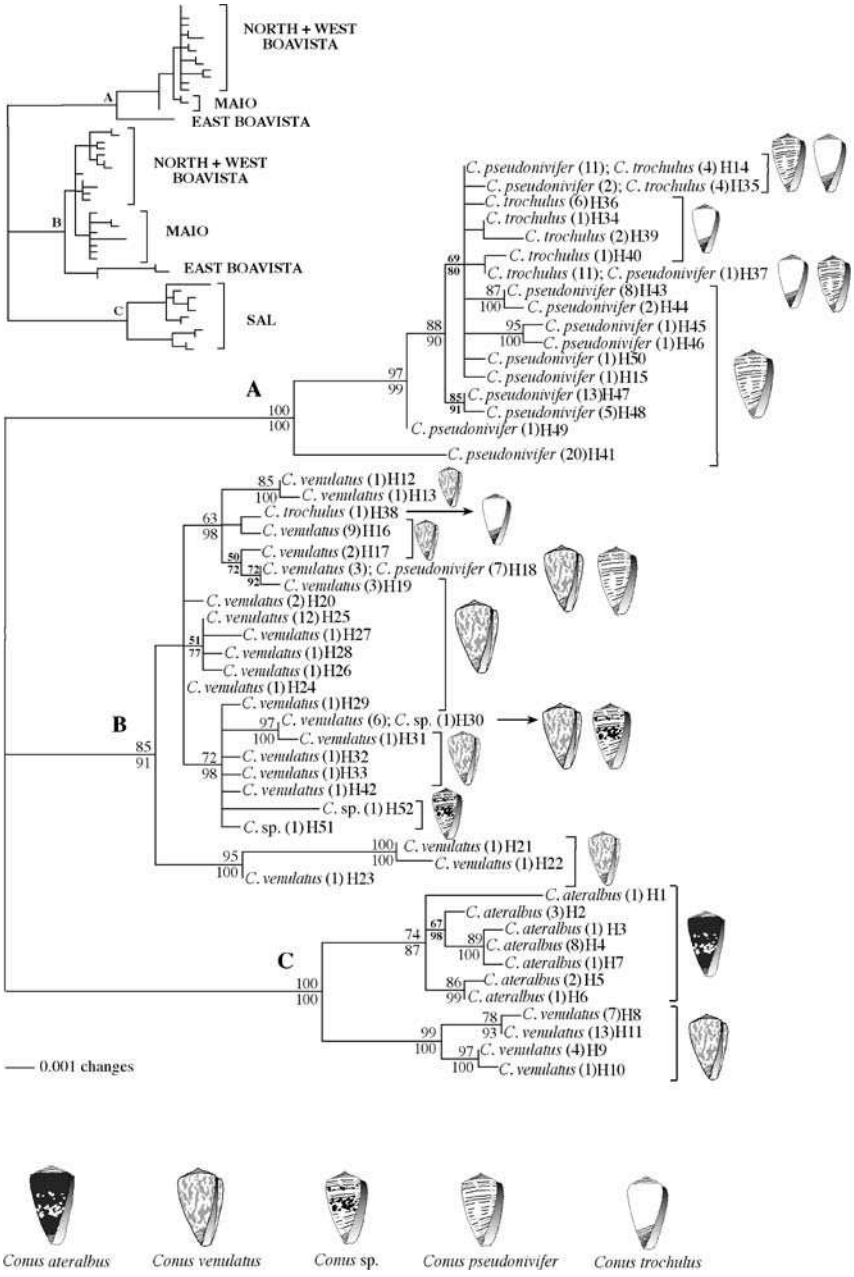

Fig. 2 Phylogenetic relationships within large-shelled *Conus* from the Cape Verde archipelago. The unrooted ML (TrN + I) tree based on mitochondrial *cox1* and *nad4* sequence data is shown. Numbers in brackets represent the number of specimens sequenced per haplotype. Numbers above and below nodes correspond to ML bootstrap and BI posterior probability values, respectively. Shell banding patterns are mapped onto the phylogeny. The inset shows phylogeographical patterns of diversification within the large-shelled *Conus* from Cape Verde.

this clade were generally unresolved. Interestingly, some specimens with *C. pseudonivifer* and *C. trochulus* shell banding phenotypes shared the same haplotype. Clade B (85% BP and 91% BPP) is mostly composed of haplotypes corresponding to a *C. venulatus* shell banding phenotype, although the following exceptions occur: (i) one specimen with a *C. trochulus* shell banding phenotype, i.e. H38, (ii) seven specimens with a *C. pseudonivifer* shell banding phenotype (that share one haplotype, i.e. H18, which is also found in three specimens with a *C. venulatus* shell banding phenotype), and (iii) three nondetermined specimens (*Conus* sp.) each with a different haplotype (i.e. H30, H51 and H52, being the first one shared also by six specimens with a *C. venulatus* shell banding phenotype) that showed an intermediate shell banding phenotype between those assigned to *C. venulatus* and *C. pseudonivifer*. Clade C is supported by maximal BP and BPP values, and includes two distinct groups, one including specimens with *C. venulatus* shell banding phenotypes, and the other comprising specimens with a *C. ateralbus* shell banding phenotype. Divergence date (and corresponding confidence intervals) of the three main clades from their most recent common ancestor was estimated to be 3.93 Ma (2.37, 7.56) following a Bayesian 'relaxed-clock' approach.

Phylogeographical patterns

The phylogeography of Cape Verde *Conus* is schematically depicted in the inset of Fig. 2. Almost all specimens grouped into clade C are from Sal (except two specimens sharing haplotype H11 from northern Boavista). Clades A and B showed a repeated phylogeographical pattern. Populations from northwestern Boavista and Maio consistently grouped together to the exclusion of eastern Boavista populations. The exceptions to this general phylogeographical pattern were the following: (i) in clade A, 10 specimens (one included in H37, eight belonging to H14, and one that is H50) with a *C. pseudonivifer* shell banding phenotype from Maio were recovered together with northern and western Boavista populations; (ii) in clade B, three specimens with a *C. venulatus* shell banding phenotype (two sharing H20, and one that is H24) from eastern Boavista clustered with populations from northwestern Boavista. One specimen with a *C. venulatus* shell banding phenotype (i.e. H42) from eastern Boavista grouped with populations from Maio; and (iii) in clade C, two specimens with a *C. venulatus* shell banding phenotype from northern Boavista (included in H11) grouped together with populations showing a *C. venulatus* shell banding phenotype from Sal.

Haplotype network analysis

In order to further understand haplotype diversity and genealogy, a statistical parsimony network was reconstructed for clades A, B, and C, individually (Fig. 3). Clade A with 96 specimens grouped into 17 haplotypes, displayed an intermediate level of haplotype and nucleotide diversities (0.888 ± 0.014 and 0.0045 ± 0.0004, respectively). Clade B with 62 specimens, and 24 haplotypes showed higher haplotype and similar nucleotide diversities (0.909 ± 0.019 and 0.0041 ± 0.0004, respectively). Clade C with 42 specimens and 11 haplotypes showed the lowest haplotype (0.841 ± 0.034) and highest nucleotide diversities (0.0066 ± 0.0004). Clade A network has a diffuse star-like shape, where the central and highly abundant ancestral haplotype (H14) is connected to all but one derived haplotypes by one to four mutation steps. The most frequent haplotype (H41) is connected to the ancestral haplotype by 16 mutation steps, below the 95% statistical confidence limit. Clade B network is characterized by a less abundant ancestral haplotype (H24) connected to derived haplotypes by one to 16 nucleotide substitutions. Ancestral haplotype (H11) from clade C is the single most abundant, but peripheral haplotype in a network that displays a clear subdivision between two groups: specimens with *C. venulatus* phenotype are separated at least by 14 mutation steps from specimens with *C. ateralbus* phenotype. The proportion of specimens with unique haplotypes is much higher in clade B (71%) than in clades A (41%), or C (46%).

Population genetic structure

Significant levels of genetic structuring were found within clade A ($\Phi_{ST} = 0.92$; $P < 0.001$) and clade B ($\Phi_{ST} = 0.57$, $P < 0.0001$) populations. Levels of genetic differentiation among populations of clades A and B were examined within and between Boavista and Maio islands. Populations of clade A showed strong genetic structuring within ($\Phi_{SC} = 0.92$, $P < 0.001$) but not between ($\Phi_{CT} = 0.02$, $P = 0.24$) islands. Populations of clade B showed strong genetic structuring both within ($\Phi_{SC} = 0.47$, $P < 0.001$) and between ($\Phi_{CT} = 0.36$, $P < 0.01$) islands. Further AMOVA tests were performed to probe whether there is genetic structuring between northwestern and eastern Boavista populations, as suggested by the reconstructed molecular phylogeny. Strong genetic structuring among Maio, northwestern and eastern Boavista populations was found both for clade A ($\Phi_{CT} = 0.79$, $P < 0.01$) and clade B ($\Phi_{CT} = 0.39$, $P < 0.001$).

Geometric morphometrics of shell and radula shapes

Since shell colour and banding patterns were found to be unreliable predictors of species taxonomic status, we performed geometric morphometrics of shell and radula shapes. We compared groups as defined by shell phenotype (*C. ateralbus*, *C. venulatus*, *C. trochulus* and *C. pseudonivifer*), and by island (Sal, Boavista and Maio). In addition, the hypothesis of an effective correlation between morphological features of the shell or of the radula, and the clades recovered in the molecular phylogeny was tested with a one-way MANOVA on the landmark coordinates using Procrustes metrics, and the following five clades inferred in the phylogenetic analysis: (i) *Conus* from Sal island, (ii) *C. venulatus* from Maio and northwestern Boavista, (iii) *C. venulatus* from eastern Boavista, (iv) *C. pseudonivifer* from Maio, and *C. pseudonivifer* and *C. trochulus* from northwestern Boavista, and (v) *C. pseudonivifer* from eastern Boavista. The results of the one-way MANOVA tests for shell and radular shape data using three different grouping criteria are shown in Table 4. Shell shape data explained low percentages of the variance regardless of the grouping factor. Apparently, there is little correlation between shell shape data and the clades recovered from the molecular analysis. In fact, CVA of the shape of 174 shells (partial warp scores) using shell phenotype as grouping factor showed large overlapping of the clusters of points corresponding to each of the groups (Fig. 4). The pairwise Procrustes distances based upon shell morphometry between the different groups are in general small or very small, although statistically significant (Table S1, Supplementary material). CVA of the shape of shells using locality (island) or clades as grouping factors rendered essentially nonsignificant results. Principal component analysis (PCA) of shell morphology rendered similar results and no groupings showed differences (not shown).

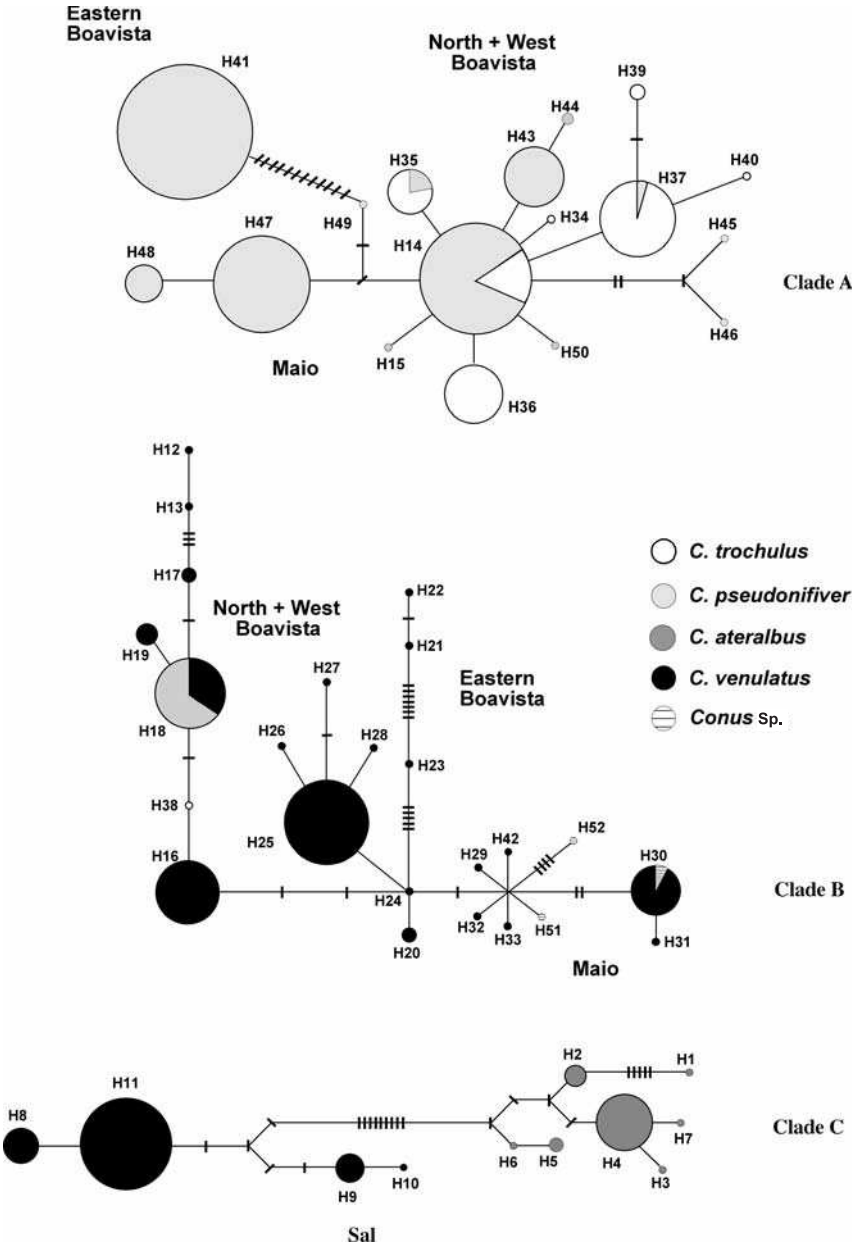

Fig. 3 TCS parsimony networks were performed independently for each clade recovered in the phylogenetic analyses. Pairwise distance values for all haplotypes were estimated defining the limits of parsimony in constructing networks above the 95% level. The only exception is clade A in which this limit was set to 90% due to the higher number of mutation steps needed to connect haplotype H41. Shell banding phenotypes are denoted by different grey patterns. Missing haplotypes are depicted as vertical bars.

According to the one-way MANOVA tests, radular shape data explained the largest percentages of the variance when shell phenotype and clade (but not island) were used as grouping factors (Table 4). CVA of the shape data (partial warp scores) of the entire data set of 107 radular teeth was also performed. All radular teeth examined were of the vermivorous type. Principal components (PC) 1 and 2 had statistically significant eigenvalues, which accounted for 85.4% of the variance in the shape data. PC1 represents the relative shortening of the radular tooth along its axis, with most of the change being concentrated around the waist. This component alone accounted for 79.8% of the variance in the shape data. Along this axis, the separation of the teeth into two large groups was evident from a 2D scatter plot (not shown). Radular teeth of specimens assigned either to *C. trochulus* or *C. pseudonivifer* were significantly more elongated and more slender than those of specimens identified as *C. ateralbus* or *C. venulatus*. PC2 represents a curved deformation consistent with the bending of the radular tooth. CVA of the radular shape data considering shell phenotype (taxon) as grouping factor yielded the 2D scatter plot shown in Fig. 5 (pairwise Procrustes distances between these groups based upon radular tooth morphometry are listed in Table S2, Supplementary material). The separation of *C. ateralbus* and *C. venulatus* from *C. pseudonivifer* and *C. trochulus* is evident along CV1, which

Table 4 Results of the one-way MANOVA using three different grouping criteria

Grouping factor	Explained SS†	Unexplained SS	% explained	*F*‡	*P*‡
A) Shell shape					
Shell type	0.0336	0.1881	15.135	10.10	0.002
Island	0.0065	0.2152	2.919	2.57	0.006
Clade	0.0121	0.2096	5.455	2.44	0.002
B) Radula shape					
Shell type	0.2418	0.1394	63.42	59.53	0.002
Island	0.0556	0.3255	14.60	8.89	0.002
Clade	0.2580	0.1232	67.68	53.40	0.002

†SS, sum of squares.
‡Significance is assessed by a bootstrapped *F*-test (500 bootstraps).

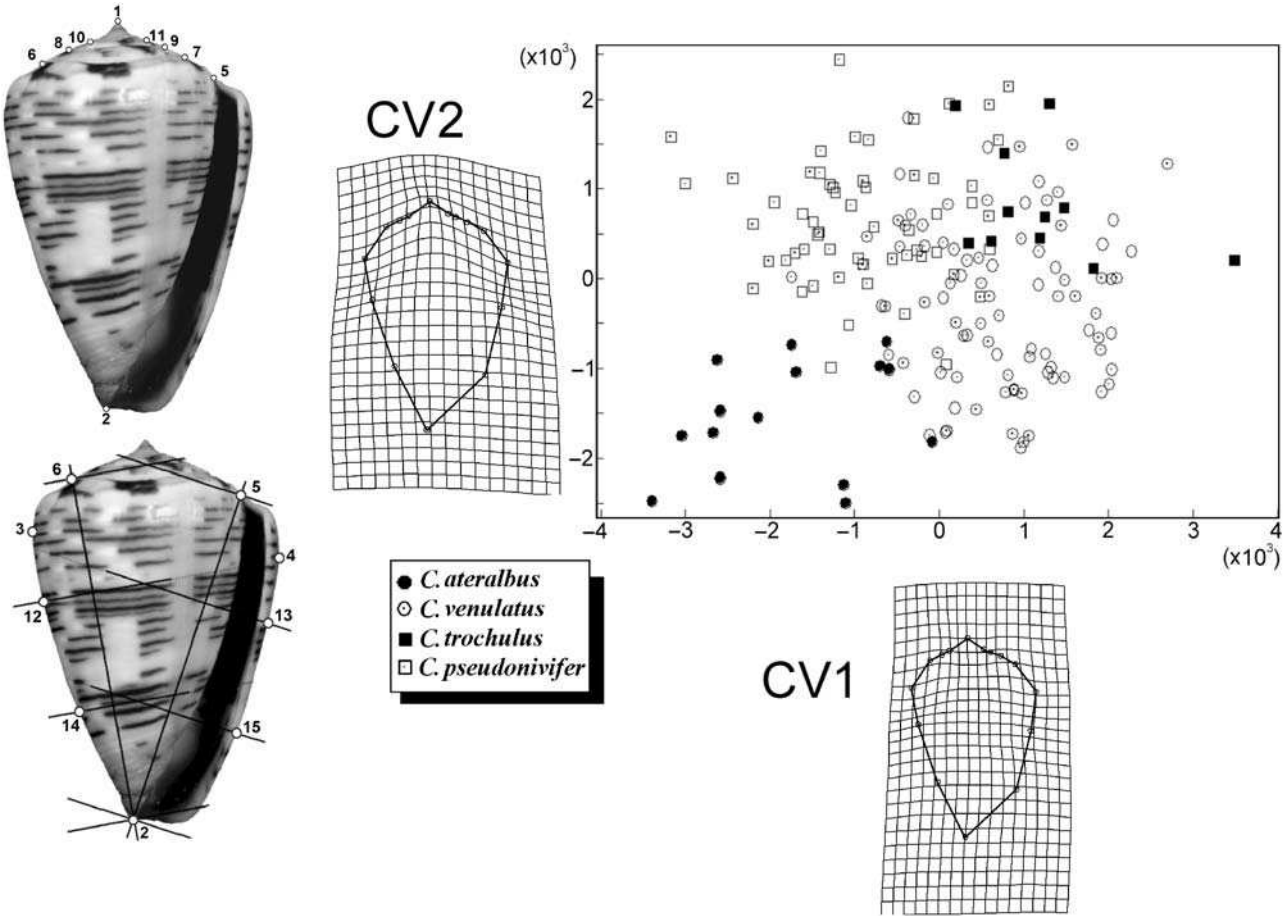

Fig. 4 Canonic variate analysis (CVA) of the shape of the shell of 174 specimens corresponding to 15 populations belonging to the large-shelled clade of Cape Verde *Conus*, considering shell type (taxon) as grouping factor. The 2D scatter plot of the CVA, and the corresponding deformation grids and vectors are shown. The numbers in the upper and lower shells are landmarks and semilandmarks (see Table 3), respectively. CV1 represents the sharpening of the spire tip and siphonal channel and the narrowing of the last whorl with the concomitant descent of the points marking the maximum width of the shells. CV2 represents the increase in the spire height and changes towards a more cylindrical last whorl.

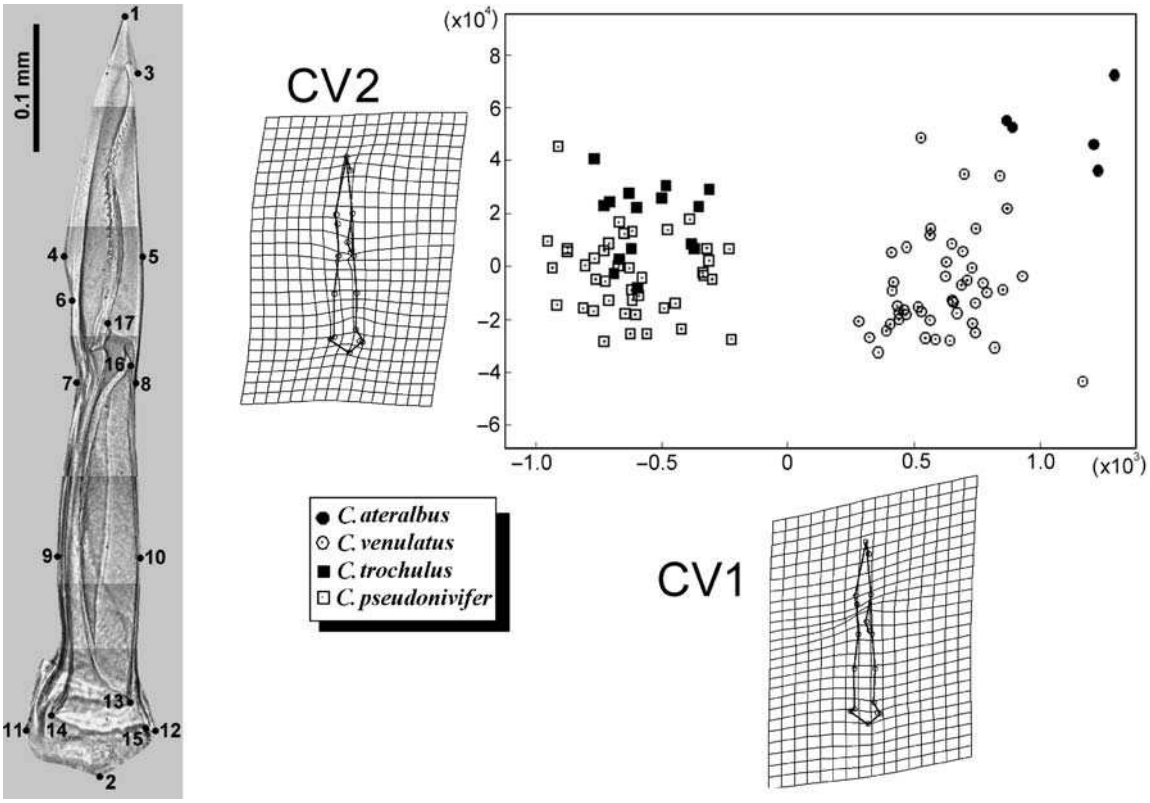

Fig. 5 Canonic variate analysis (CVA) of the shape of 107 radular teeth from 21 populations belonging to the large-shelled clade of Cape Verde *Conus*, considering shell phenotype (taxon) as grouping factor. The 2D scatter plot of the CVA, and the corresponding deformation grids and vectors are shown. The numbers in the radular tooth represent landmarks and semilandmarks used in the morphometric analyses (see Table 3). CV1 represents the relative shortening of the radular tooth along its axis. CV2 represents a curved deformation consistent with the bending and relative broadening of the radular tooth.

represents essentially the same deformation implied by PC1. Furthermore, specimens of *C. ateralbus* are separated from *C. venulatus* along CV2, but there is a large overlapping between *C. pseudonivifer* and *C. trochulus*. Using these CV axes, 17 out of 107 specimens were misclassified (84.1% correct). A total of 13 of the misclassified specimens were either *C. pseudonivifer* or *C. trochulus*, whereas only four *C. venulatus* were misclassified as *C. ateralbus*. CVA of the radular shape data considering general locations (islands) as grouping factor yielded a 2D scatter plot, in which all point overlapped (not shown; the corresponding pairwise Procrustes distances are listed in Table S3, Supplementary material). CVA of the radular shape data considering clade as grouping factor yielded the 2D scatter plot shown in Fig. 6 (the corresponding pairwise Procrustes distances are listed in Table S4, Supplementary material), which represents a useful insight on the correlation between radular morphometry and molecular data. Clades 4 and 5 (as defined above) were well resolved, and separated from clades 1, 2 and 3. Using the CV1 and CV2 axes, only five out of 107 specimens were misclassified (95.3% correct assignment). Similar results were obtained when only three clades (A, B and C) were considered (CVA/MANOVA: 96.2% correct assignments, 63.2% variance explained, $F = 89.46$, $P < 0.002$; not shown). PCA of radular morphology rendered similar results and only groupings recovered in the molecular phylogeny showed significant differences (not shown).

Discussion

Evolution of shell colour and banding patterns and taxonomic implications

The variation in shell colour and banding patterns has been traditionally used as the main phenotypic character to classify large-shelled *Conus* from Cape Verde into species (Röckel *et al*. 1980). However, comprehensive surveys of large-shelled *Conus* in the archipelago reveal a remarkable diversity of shell banding patterns at the population level (Monteiro *et al*. 2004; this study), which certainly complicates unambiguous species taxonomic assignment. The reconstructed molecular phylogeny and networks of large-shelled *Conus* revealed three well-defined clades that do not correspond to current species classification based on shell colour and

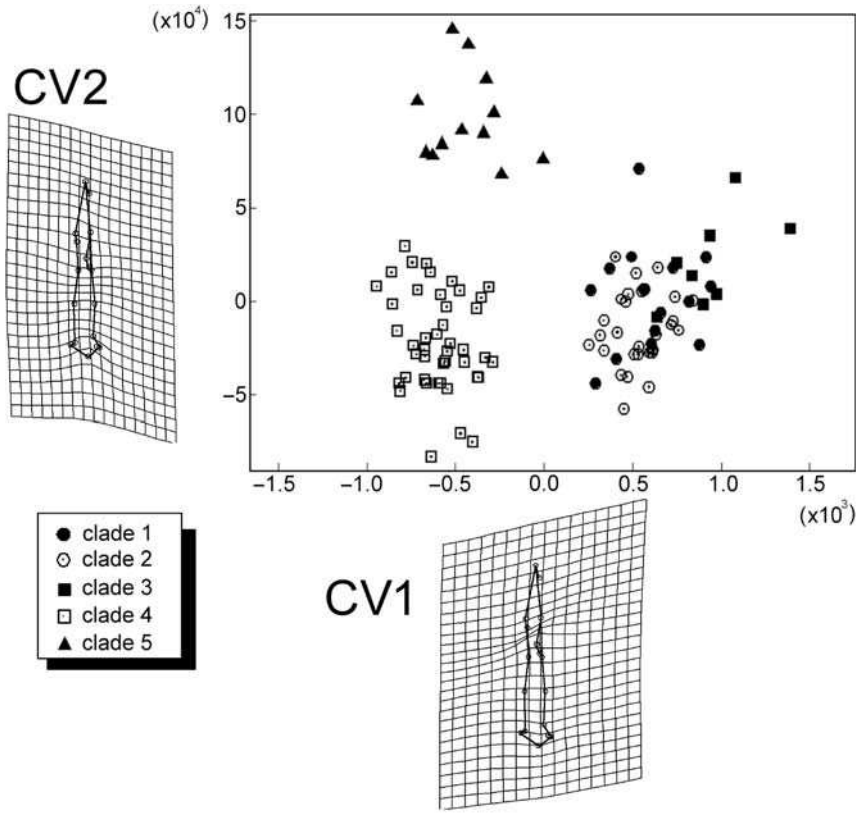

Fig. 6 Canonic variate analysis (CVA) of the shape of 107 radular teeth from 21 populations belonging to the large-shelled clade of Cape Verde *Conus*, considering clade as grouping factor. The 2D scatter plot of the CVA, and the corresponding deformation grids and vectors are shown. Clades were defined based on the molecular tree as follows: clade 1, *Conus* from Sal island; clade 2, *C. venulatus* from Maio and northern and western Boavista; clade 3, *C. venulatus* from eastern Boavista; clade 4, *C. pseudonivifer* from Maio; and *C. pseudonivifer* and *C. trochulus* from northern and western Boavista; and clade 5, *C. pseudonivifer* from eastern Boavista.

banding patterns, and seriously question the taxonomic usefulness of these phenotypic characters. Although shell colour and banding pattern polymorphisms in gastropods are usually associated with mimicry and camouflage against predation (Cain & Sheppard 1954), their exact function in *Conus*, and whether they are under selection remain unknown. In any case, according to our morphometric analyses, it seems that subtle shell shape features may have some discriminating utility for taxonomic purposes, particularly for separating shells of *C. ateralbus* from those of other taxa.

Both mitochondrial haplotype and radular morphological data support that *C. trochulus* and *C. pseudonivifer* conform a single monophyletic group (clade A) and cannot be discerned as separate taxa. Within clade A, some specimens with either *C. trochulus* or *C. pseudonivifer* shell banding phenotypes share identical haplotypes supporting the hypothesis that the observed phenotypes may represent species polymorphism. Instances of haplotype sharing are also found in clade B. In one case, specimens with *C. venulatus* or *C. pseudonivifer* shell banding phenotypes share haplotype H18. In the other case, H30 is shared by specimens with *C. venulatus* shell banding phenotypes and one individual showing an intermediate shell banding phenotype between *C. venulatus* and *C. pseudonivifer*. In most instances, the *C. pseudonivifer* shell banding phenotype is involved in haplotype sharing, which suggests as an alternative hypothesis that the *C. pseudonivifer* shell banding phenotype could result from natural hybridization events between *C. trochulus* (clade A) and *C. venulatus* (clade B). The larger proportion of specimens with *C. pseudonivifer* shell banding phenotype in mitochondrial clade A would be best explained by a superior viability of the hybrids resulting from crossings between male *C. venulatus* × female *C. trochulus* (since mitochondrial DNA is normally maternally inherited). Hybridization in marine molluscs (Gardner 1997) is relatively common and cases of assortative fertilization and/or reduced hybrid fitness have been reported (Bierne *et al*. 2002). However, the hypothesis of a hybrid origin of *C. pseudonivifer* is contradicted both by geographical distribution patterns and radular morphological analyses. The observed wide distribution of *C. pseudonivifer* along Maio and Boavista is not expected under the hypothesis of a hybrid origin of *C. pseudonivifer*, which would instead predict a narrower distribution of the hybrid, mostly restricted to northwest Boavista, where the two putative parental species occur in sympatry. Moreover, the hypothesis of a hybrid origin of *C. pseudonivifer* would imply the existence of intermediate types between *C. trochulus* and *C. venulatus* radular morphologies. However, the close similarity in radular morphology of *C. trochulus* and *C. pseudonivifer* suggests that these taxa are most likely polymorphisms within the same species. Further phylogenetic analyses based on nuclear sequence data are needed to confirm the polymorphism hypothesis.

On the other hand, the *C. venulatus* shell banding phenotype is found both in clades B and C. The most parsimonious explanations of this phylogenetic pattern are either that the *C. venulatus* shell banding phenotype would be (i) plesiomorphic to all large-shelled *Conus* from Cape Verde; (ii) plesiomorphic only to clades B and C; and (iii) convergent and had evolved independently in clades B and C. The one-way MANOVA results indicated that each of the main recovered clades in the molecular phylogeny could be correlated with a significantly distinct radular teeth shape. Further morphological analyses searching for additional diagnostic characters are needed to determine which of the recovered clades in the molecular phylogeny may correspond to valid species.

Recurring biogeographical patterns of large- and small-shelled species of Conus

The recovered clades in the molecular phylogeny of large-shelled *Conus* show a distinctive phylogeographic pattern. In Sal, the populations form a monophyletic island assemblage (Clade C), which is in concordance with a model of *in situ* speciation. However, the situation in Maio and Boavista is quite different with populations from both islands grouped together into two clades (A and B). Within these clades a common phylogeographic pattern arises. Northern and western Boavista specimens cluster with Maio specimens to the exclusion of eastern Boavista samples. This phylogeographic pattern was further supported by the results of the AMOVA tests, which show that there is significant genetic structuring of both clades A and B populations among northwestern Boavista, eastern Boavista, and Maio. Endemic *Conus* in Cape Verde have nonplanktonic lecithotrophic larvae with limited dispersal capabilities (Strathmann 1985; Scheltema 1989), which enhance speciation by allopatry (Cunha *et al*. 2005). The recovered phylogeographic patterns as well as the significant genetic structuring of large-shelled species are in agreement with an allopatric mode of speciation. Presently, western Boavista and northern Maio are connected by a 100-m deep channel (Carta Hidrografica do Arquipélago de Cabo Verde, 1971; Instituto Hidrográfico de Lisboa), which may represent an actual physical barrier to the dispersal of shallow water nonplanktonic lecithotrophic species. However, in the Pliocene (*c*. 3.8 Ma) a low sea-level stage of –30 m (Haq *et al*. 1987, 1988) possibly constituted a bridge between both islands allowing between-island dispersal and gene flow. The origin of clades A and B was estimated 3.93 Ma, which fairly matches the mentioned period of a low sea-level stand. Although originated during the same period, clade C is exclusive of Sal. The ocean channel between Sal and the closest island of Boavista is 500 m deep (Carta Hidrografica do Arquipélago de Cabo Verde, 1971; Instituto Hidrográfico de Lisboa), which impeded the cross of nonplanktonic larvae even during low sea-level stages.

The relative role of determinism and historical contingency in shaping evolutionary processes is a fundamental question in evolutionary biology (Langerhans & DeWitt 2004). The many examples of convergence found in, e.g. island biota provide arguments in favour of the deterministic nature of evolution (Hendry & Kinnison 2001). However, it is also argued that replaying the 'tape of life' would lead inevitably to disparate evolutionary outcomes due to the existence of unique past events in the history of any lineage (Gould 1989). Here, we show that 12 Myr later, the large-shelled *Conus* of Cape Verde have remarkably replicated the biogeographical diversification patterns of small-shelled *Conus* (Cunha *et al*. 2005). Common selective forces have played a greater role than chance events in shaping biogeographical patterns of *Conus* in Cape Verde. Both taxa have nonplanktonic lecithotrophic larvae with limited dispersal capacity that impose diversification in allopatry by vicariance. The hypothesis that best explains the recurring biogeographical patterns is that changes in island coastline during low sea-level stands at the peak of successive glaciations (at 16.5 Ma and 3.8 Ma, respectively) together with similar selective forces triggered diversification of both taxa in the same manner. Hence, the two replicated events of evolutionary diversification of *Conus* in Cape Verde provide a textbook example in favour of the important role of determinism in canalizing biogeographical patterns over long periods of time.

Acknowledgements

We thank E. Rolán for helpful comments on species distribution. We are also grateful to M. Bastir and I. Doadrio for helpful comments about the morphometric analyses. Three anonymous reviewers provided insightful comments on a previous version of the manuscript. R.L.C. was supported by a PhD grant (SFRH/BD/9209/2002) from the Portuguese Foundation for Science & Technology (FCT) and partially funded by a Luso-Spanish action E-105/106 (2006–07) financed by the Portuguese University Council of Rectors (CRUP) and by the GRICES/CSIC bilateral cooperation (2004–05). The work was also funded by a grant of the Ministerio de Educación y Ciencia (CGL2007-60954) to R.Z.

References

Akaike H (1973) Information theory as an extension of the maximum likelihood principle. In: *2nd International Symposium on Information Theory* (eds Csaksi F, Petrov BN), pp. 267–281 Akademiai Kiado, Budapest, Hungary.

Barnosky AD, Koch PL, Feranec RS, Wing SL, Shabel AB (2004) Assessing the causes of Late Pleistocene extinctions on the continents. *Science*, **306**, 70–75.

Bierne NPD, Boudry P, Bonhomme F (2002) Assortative fertilization and selection at larval stage in the mussels *Mytilus edulis* and *M. galloprovicialis. Evolution*, **56**, 292–298.

Cain AJ, Sheppard PM (1954) Natural selection in *Cepaea*. *Genetics*, **39**, 89–116.

Clement M, Posada D, Crandall KA (2000) TCS version 1.17: a

computer program to estimate gene genealogies. *Molecular Ecology*, **9**, 1657–1660.

Cunha RL, Castilho R, Rüber L, Zardoya R (2005) Patterns of cladogenesis in the venomous marine gastropod genus *Conus* from the Cape Verde Islands. *Systematic Biology*, **54**, 634–650.

Doyle JJ, Doyle JL (1987) A rapid DNA isolation for small quantities of leaf tissue. *Phytochemical Bulletin*, **19**, 11–15.

Duda TFJ, Kohn AJ (2005) Species-level phylogeography and evolutionary history of the hyperdiverse marine gastropod genus *Conus*. *Molecular Phylogenetics and Evolution*, **34**, 257–272.

Duda TFJ, Rolán E (2005) Explosive radiation of Cape Verde *Conus*, a marine species flock. *Molecular Ecology*, **14**, 267–272.

Emerson BC (2002) Evolution on oceanic islands: molecular phylogenetic approaches to understanding pattern and process. *Molecular Ecology*, **11**, 951–966.

Emerson B, Oromi P, Hewitt GM (1999) mtDNA phylogeography and recent intra-island diversification among Canary Island *Calathus* beetles. *Molecular Phylogenetics and Evolution*, **13**, 149–158.

Excoffier L, Smouse PE, Quattro JM (1992) Analysis of molecular variance inferred from metric distances among DNA haplotypes — Application to human mitochondrial DNA restriction data. *Genetics*, **131**, 479–491.

Excoffier L, Laval G, Schneider S (2005) ARLEQUIN version 3.0: an integrated software package for population genetics data analysis. *Evolutionary Bioinformatics Online*, **1**, 47–50.

Folmer OM, Black W, Hoeh R, Lutz R, Vrijenhoek R (1994) DNA primers for amplification of mitochondrial cytochrome *c* oxidase subunit I from diverse metazoan invertebrates. *Molecular Marine Biology and Biotechnology*, **3**, 294–299.

Gardner JPA (1997) Hybridization in the sea. *Advances in Marine Biology*, **31**, 1–78.

Gillespie R (2004) Community assembly through adaptive radiation in Hawaiian spiders. *Science*, **303**, 356–359.

Gould SJ (1989) *Wonderful Life — The Burgess Shale and the Nature of History*. W.W. Norton & Co., New York.

Graham MH, Dayton PK, Erlandson JM (2003) Ice ages and ecological transitions on temperate coasts. *Trends in Ecology & Evolution*, **18**, 33–40.

Guindon S, Gascuel O (2003) A simple, fast and accurate algorithm to estimate large phylogenies by maximum likelihood. *Systematic Biology*, **52**, 696–704.

Haq BU, Hardenbol J, Vail PR (1987) Chronology of fluctuating sea levels since the Triassic. *Science*, **235**, 1156–1167.

Haq BU, Hardenbol J, Vail PR (1988) Mesozoic and Cenozoic chronostratigraphy and cycles of sea-level change. In: *Sea-Level Changes; An Integrated Approach: Society of Economic Paleontologists and Mineralogists, Special Publication* (eds Wilgus CK, Hastings BS, Ross CA, Posamentier H, Van Wagonar J, Kendall CGStC), **42**, 71–108.

Hendry AP, Kinnison MT (2001) An introduction to microevolution: rate, patterns, process. *Genetica*, **112–113**, 1–8.

Hewitt GM (2000) The genetic legacy of the quaternary ages. *Nature*, **405**, 907–913.

Huelsenbeck JP, Crandall KA (1997) Phylogeny estimation and hypothesis testing using maximum likelihood. *Ecological Systematics*, **28**, 437–466.

Jordan S, Simon C, Foote D, Englund RA (2005) Phylogeographic patterns of Hawaiian *Megalagrion* damselflies (Odonata: Coenagrionidae) correlate with Pleistocen island boundaries. *Molecular Ecology*, **14**, 3457–3470.

Kishino H, Thorne JL, Bruno WJ (2001) Performance of a divergence time estimation method under a probabilistic model of rate evolution. *Molecular Biology and Evolution*, **18**, 352–361.

Kohn AJ, Nishi M, Pernet B (1999) Snail spears and scimitars: a character analysis of Conus radular teeth. *Journal of Molluscan Studies*, **65**, 461–481.

Kohn AJ, Riggs AC (1975) Morphometry of the *Conus* shell. *Systematic Zoology*, **24**, 346–359.

Langerhans RB, DeWitt TJ (2004) Shared and unique features of evolutionary diversification. *American Naturalist*, **164**, 335–349.

Leviten PJ (1978) Resource partitioning by predatory gastropods of the genus *Conus* on subtidal Indo-Pacific coral reefs: the significance of prey size. *Ecology*, **59**, 614–631.

Losos JB (2004) Adaptation and speciation in Greater Antillean anoles. In: *Adaptive Speciation* (eds Dieckmann U, Doebeli M, Metz JAJ, Tautz D), pp. 335–343. Cambridge University Press, Cambridge, UK.

Millien-Parra V, Jaeger JJ (1999) Island biogeography of the Japanese terrestrial mammal assemblages: an example of a relict fauna. *Journal of Biogeography*, **26**, 959–972.

Monteiro A, Tenorio MJ, Poppe GT (2004) *The Family Conidae. The West African and Mediterranean Species of* Conus. Conchbooks, Hackenheim, Germany.

Posada D (2004) COLLAPSE 1.2. Available at: http://darwin.uvigo.es/software/collapse.html.

Posada D, Crandall KA (1998) MODELTEST: testing the model of DNA substitution. *Bioinformatics*, **14**, 817–818.

Richman AD, Case TJ, Schwaner TD (1988) Natural and unnatural extinction rates of reptiles on islands. *American Naturalist*, **131**, 611–630.

Röckel D, Rolán E, Monteiro A (1980) *Cone Shells from Cape Verde Islands, a Difficult Puzzle*. Feito, Vigo.

Rohlf FJ (2005) TPSDIG version 2.04 and TPSRELW version 1.42. Available at: http://Life.Bio.SUNYSB.edu/morph/morph.html, Stony Brook, NY 11794-5245.

Rolán E (1992) *La familia Conidae (Mollusca, Gastropoda) en el archipiélago de Cabo Verde (Africa Occidental)*. PhD, Universidade de Santiago.

Rolán E, Raybaudi-Massilia G (1994) New investigation on the radular teeth of *Conus* (Prosobranchia: Conidae). Part I. *Argonauta*, **8**, 6–59.

Rolán E, Raybaudi-Massilia G (2002) Evaluation of character state polarity of *Conus* radular tooth characters. *Bollettino Malacologico*, **4**, 175–194.

Ronquist F, Huelsenbeck JP (2003) Bayesian phylogenetic inference under mixed models. *Bioinformatics*, **19**, 1572–1574.

Rozas J, Sánchez-DelBarrio JC, Messeguer X, Rozas R (2003) DNASP, DNA polymorphism analysis by the coalescent and other methods. *Bioinformatics*, **19**, 2496–2497.

Scheltema RS (1989) Planktonic and non-planktonic development among prosobranch gastropods and its relationship to the geographic range of species. In: *Reproduction, Genetics and Distribution of Marine Organisms* (eds Ryland JS, Tyler RA), pp. 183–188. Olsen & Olsen, Fredensborg, Denmark.

Sheets HD (2003–2005) *IMP-Integrated Morphometrics Package* (ed. Department of Physics CC), 2001 Main St, Buffalo, NY 14208, 716-888-2587.

Strathmann RR (1985) Feeding and nonfeeding larval development and life-history evolution in marine invertebrates. *Annual Review in Ecology and Systematics*, **16**, 339–361.

Swofford D (1998) PAUP* *Phylogenetic Analysis Using Parsimony (* and Other Methods)*. Sinauer Associates, Sunderland, Massachusetts.

Taberlet P, Fumagalli L, Wust-Saucy A-G (1998) Comparative phylogeography and postglacial colonization routes in Europe. *Molecular Ecology*, **7**, 453–464.

Templeton AR, Crandall KA, Sing CF (1992) A cladistic analysis of phenotypic associations with haplotypes inferred from restriction endonuclease mapping and DNA sequence data. III. Cladogram estimation. *Genetics*, **132**, 619–633.

Thompson JD, Gibson TJ, Plewniak F, Jeanmougin F, Higgins DG (1997) The CLUSTAL_X Windows interface: flexible strategies for multiple sequence alignment aided by quality analysis tools. *Nucleic Acids Research*, **24**, 4876–4882.

Zelditch ML, Swiderski DL, Sheets HD, Fink WL (2004) Geometric Morphometrics for Biologists: a Primer. Elsevier Academic Press, London, p. 437.

Regina L. Cunha is a Ph.D. student in the Department of Evolutionary Biology and Biodiversity at the Museo Nacional de Ciencias Naturales-CSIC, Madrid, Spain, where her research interest has focused on the evolutionary biology of marine snails on oceanic islands. Manuel J. Tenorio is interested in the research on the family Conidae as a whole, and particularly the species from the Western African coast and Islands. He is also interested in the application of geometric morphometric techniques to the study of Conidae and of other molluscs families, both marine and terrestrial. Carlos Afonso is interested on the systematic, biology and bio-distribution of benthic macro-fauna found in the Algarve coast, as well as, the classification and systematic revision of the gastropods of the genus *Conus* in the Cape Verde Archipelago. Rita Castilho is interested in population genetics and phylogeography in an array of different organisms. Rafael Zardoya is interested in understanding the evolutionary mechanisms that are involved in the generation of biodiversity. His research is currently focused on establishing a robust phylogenetic framework for gastropods.

Supplementary material

The following supplementary material is available for this article:

Table S1 Pairwise Procrustes distances between groups of specimens as defined by shell phenotype (taxon), based upon shell morphometry

Table S2 Pairwise Procrustes distances between groups of specimens defined by shell phenotype (taxon), based upon radular morphometry

Table S3 Pairwise Procrustes distances between groups of specimens defined by location (island), based upon radular morphometry

Table S4 Pairwise Procrustes distances between groups of specimens defined by clade, based upon radular morphometry

This material is available as part of the online article from:
http://www.blackwell-synergy.com/doi/abs/10.1111/j.1365-294X.2007.03618.x
(This link will take you to the article abstract).

Please note: Blackwell Publishing are not responsible for the content or functionality of any supplementary materials supplied by the authors. Any queries (other than missing material) should be directed to the corresponding author for the article.

Appendix

Number of specimens examined per population in the morphometric analysis of radular teeth

Taxon	Island	Location	No. of specimens
Conus ateralbus	Sal	Calheta Funda	5
C. venulatus	Sal	Rabo de Junco	5
C. venulatus	Sal	Serra Negra	5
C. venulatus	Boavista	Sal Rei	5
C. venulatus	Boavista	Praia de Canto	8
C. venulatus	Boavista	Derrubado 4	5
C. venulatus	Boavista	Derrubado 3	5
C. venulatus	Maio	Pau Seco	4
C. venulatus	Maio	Porto Cais	4
C. venulatus	Maio	Praia Real	5
C. trochulus	Boavista	Sal Rei	3
C. trochulus	Boavista	Morro de Areia	4
C. trochulus	Boavista	Teodora	5
C. trochulus	Boavista	Ervatão	3
C. pseudonivifer	Boavista	Porto Ferreira	5
C. pseudonivifer	Boavista	Morro de Areia	3
C. pseudonivifer	Boavista	Derrubado 4	5
C. pseudonivifer	Boavista	Ponta do Sol	6
C. pseudonivifer	Boavista	Praia de Canto	7
C. pseudonivifer	Maio	Pau Seco	7
C. pseudonivifer	Maio	Praia Real	8
Total			107